Chapter 6

Space Weather and Climate

The term Space Weather denotes variations of the Earth's environment on short terms. In analogy to meteorology, where the distinction between weather and climate is made, space climate denotes long term variations of the Earth's climate mainly caused by solar variations.

6.1 The Atmosphere's Response to Solar Irradiation

6.1.1 Introduction

The penetration of solar radiation strongly depends on its wavelength, the larger the wavelength the deeper the penetration (see Fig. 6.1).

The principal effects of solar radiation on the middle and upper atmosphere are summarized in table 6.1. In the second and the third column of that table the variation due to the solar activity cycle is given. From that table it follows that the amount of variation depends on the wavelength of the solar radiation becoming smaller at longer wavelengths. Above 300 nm it is very difficult to detect and can be measured only with satellite radiometric detectors.

In addition to radiation, the Sun also emits the solar wind which consists of particles that interact with the geomagnetic field to form the Earth's magnetosphere. We observe a large input of electrons and protons (causing the aurora) and ionospheric currents are produced causing joule heating. In principle these phenomena are concentrated at high geomagnetic latitudes; heating effects can spread equatorward by convection and conduction.

The typical structure of the Earth's atmosphere was already shortly described. The boundaries of the various layers (Troposphere, Stratosphere, Mesosphere, Ionosphere) are called pauses (e.g. the Tropopause) and are defined by minima or maxima of the temperature profile. At 100 km the density is 10^{-6} of its surface value. The temperature in the thermosphere is strongly dependent on solar activity. The major sources for heating at this layer are:

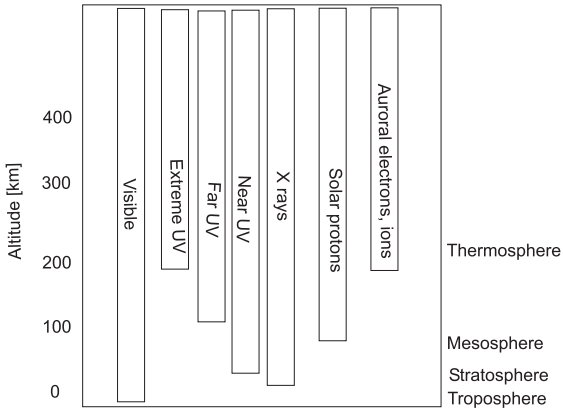

Figure 6.1: Penetration of different solar light waves resp. their induced particles in the atmosphere

Table 6.1: Effects of Solar Radiation at different wavelengths on the Middle and Upper Atmosphere.

Wavelength [nm]	Variab. middle Atm.	Variab. upper Atm.	Effect	Height [km]
1-10, SXR		sporadic	Ion. all	70-100
10-100, XUV	2ppm	2 x	Ion. N_2, O, O_2	
100-120, EUV	6 ppm	30%	Ion. NO	80-100
120-200, VUV	150 ppm	10%	Diss. O_2	40-130
200-240, UV	0.12%	5%	Diss. O_2, O_3	20-40
240-300, UV	1.0%	<1%	Diss. O_3	20-40

- solar ionizing photons,
- magnetospheric processes.

The principal part of the ionosphere is produced by XUV which is strongly absorbed there. Ionization and recombination occurs and this contributes to the heating of the thermosphere. By comparing with table 6.1 we see that the energy involved is small; dissociation of O_2 is strong, above 120 km oxygen occurs as atoms. Through vertical mixing the ratio $O_2 : N_2$ is constant near 0.1 throughout the lower thermosphere. Oxygen atoms are produced down to 30 km and most of them combine with O_2 to form ozone. This attains a peak ratio of 10^{-5} near 30 km. Photons around 300 nm can reach the surface. They produce electronically excited oxygen and surface ozone which drives a large fraction of urban pollution chemistry.

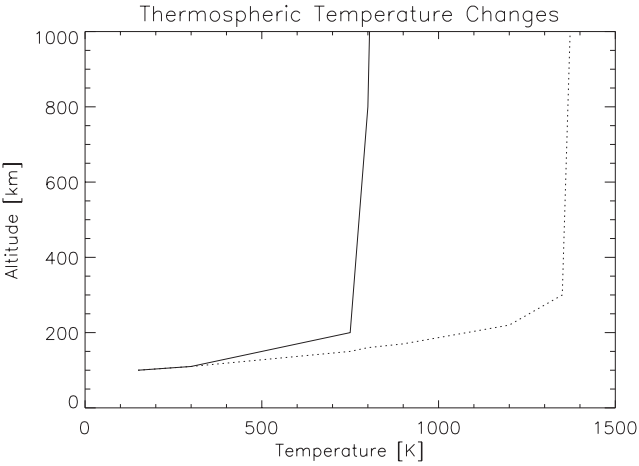

Figure 6.2: Thermospheric temperature changes, a) low solar activity, $F_{10.7} = 80, A_p = 0$, b) high solar activity, $F_{10.7} = 200, A_p = 80$ (dashed line). F10.7 denotes the 2800 MHz solar flux which is a measure for solar activity, the Ap index is a measure of the general level of geomagnetic activity over the globe. Up to the top of the troposphere the two curves are nearly identical. At a height of about 100 km the difference is already of the order of several 10 K.

6.1.2 UV Radiation

Solar radiation shortward 320 nm represents only 2% of the total solar irradiance; 0.01% of the incident flux is absorbed in the thermosphere at about 80 km and 0.2% in the stratosphere above 50 km. This radiation is extremely important since the thermal structure and photochemical processes above the troposphere are controlled by it. The stratosphere is controlled by absorption and dissociation of O_2 in the 175 to 240 nm range. The 205 to 295 nm range is predominantly absorbed by ozone O_3. If there is a stratosphere- troposphere coupling, this could affect also the climate. The short term variation of UV radiation is ascribed to the evolution and rotation of plage regions on the solar disk. The XUV induced thermospheric temperature changes is shown for low and high solar activity in Fig. 6.2. Solar activity is measured in terms of the 10.7 cm radio flux and of the plage area A_p.

6.1.3 Energetic Particles

There are three main contributions:

- electrons: they reach the high latitude thermosphere after interaction with the geomagnetic field and acceleration;
- high energy solar protons: their flux is enhanced during periods of large flares;

Table 6.2: Exospheric temperature at solar maximum and minimum

	Temperature of exosphere
solar minimum	700 K
solar maximum	1200-1500 K

- galactic cosmic rays: they originate from outside the heliosphere but their input on Earth is partly controlled by solar activity.

During large flares, intense fluxes of energetic protons (10...10^4 MeV) penetrate the Earth's polar cap regions. They produce ionization between 100 and 20 km. Such an event can last for a few hours to a few days. Large numbers of NO_x molecules are produced leading to a subsequent ozone depletion.

Relativistic electron precipitation are possible sources for ionization and odd nitrogen production at altitudes above 80 km, thus well above the ozone layer.

6.1.4 Thermosphere and Exosphere

The thermosphere starts at a height of about 90 km and ends at about 250 km at the so called exobase. In the thermosphere the temperature gradient is positive, in the exosphere collisions become negligible, particles execute ballistic orbits. The most important heat source is solar XUV radiation creating the ionosphere. The resulting heating is conducted down to the mesopause where it can be radiated. The exosphere is approximately isothermal because it lies above the level where most of the energy is deposited. Also the thermal time constant is very short because of the low density there.

The variations can be divided into diurnal variations and longer term variations.

- The diurnal variations show a day/night ratio of 1.28 over the equator with the peak occurring about 2 p.m. During the night, heat is conducted down from the top of the thermosphere to its base, the mesopause, where it is radiated.

  The effect of the sun can be expressed and measured by the 10.7 cm radio flux which is given in the units $10^{-22}\,\mathrm{Wm^{-2}Hz^{-1}}$. If this quantity is multiplied by a factor of 1.8 deg per unit of flux, we obtain the temperature.

- The other variation comes from the solar activity cycle (see Table 6.2).

The thermospheric temperature changes are illustrated in Fig. 6.2. Similarly the peak electron density varies by a factor of 2 which is very important for short-wave radio communication. The temperature changes are obtained from the 10.7 index with a multiplier of 3.6. This value is twice than that for the 27 day variation which is due to solar rotation. The difference may result from the fact that in the case of activity cycle variations not only the variation of XUV but also a

contribution from auroral heating- which is triggered by the solar wind- must be taken into account.

Finally we have to stress that both UV and particle precipitation have chemical effects and the most important is the production of N, NO and NO_2 (which is collectively called NO_x). The following reactions define the NO_x production in the thermosphere:

$$O^+ + N_2 \rightarrow NO^+ + N \quad (6.1)$$
$$N_2^+ + O \rightarrow NO^+ + N \quad (6.2)$$
$$N_2^+ + e^- \rightarrow N + N \quad (6.3)$$
$$NO^+ + e^- \rightarrow N + O \quad (6.4)$$

6.1.5 Mesosphere and Stratosphere

This region extends from the tropopause to the mesopause, at approximately 90 km. It is in local radiative equilibrium except from heat flowing in from the thermosphere. The radiative heating is by absorption of planetary radiation mainly by:

- CO_2 at 15 μm,
- O_3 at 6.3 μm
- absorption of solar UV by O_3.

The CO_2 band is the principal radiator. The O_3/CO_2 ratio decreases upwards; thus the heating to cooling also decreases and the temperature gradient is negative. In the stratosphere ozone begins to be more and more attenuated, a temperature maximum at 50 km occurs, the stratopause.

The solar UV flux is not variable at large scales thus the temperature changes to be expected from a variation of that flux should also be small. Most effects therefore come from ionization and a changing chemistry. The changes of the UV flux from the sun have only a modest effect on ozone amounts because both production (by a photolysis of O_3) and destruction are affected in the same way. Another effect is the penetration of solar protons or relativistic electrons into the middle atmosphere. By that penetration considerable amounts of NO_x are produced; these enhancements of NO_x increase the destruction of ozone at high altitudes. This could explain the inverse correlation of ozone amounts with solar activity found by Ruderman and Chamberlain (1975 [264]). Chakrabarty, 1982 [61] studied how Ozone is affected by solar proton events. During such events NO is produced that destroys ozone.

To test these predictions it is important to have data at the time scale of the solar cycle; however we must also take into account the instrumental drifts as well as the typical lifetime of the instruments which normally are below 5 yr. In the stratosphere, the ozone response is caused primarily by changes in production from O_2 and has a maximum value of 0.5 % for a 1 % change in the UV at 205 nm. The study of the response of the temperature has been made by Hood (1986

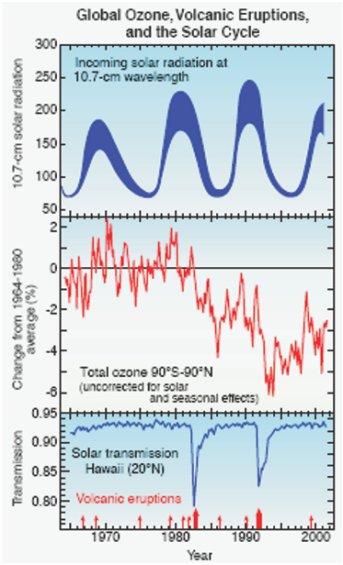

Figure 6.3: Relation between global ozone, solar activity (measured by 10.7 cm radiation) and volcanic eruptions (El Chichon, 1982, Mt. Pinatubo, 1991). Large volcanic eruptions decrease solar transmission and the particles enhance ozone depletion. Adapted from D.W.Fahey *http : //www.epa.gov/ozone/science/unep5ciQandA.pdf*

[136], 1987 [137]) and Keating *et al.* (1987 [157]) between 30 and 0.2 mbar (24 to 60 km) and later by Clancy and Rusch (1989 [68]) up to 90 km. They establish the already mentioned 0.5 % response. The very small temperature response lags the UV by 4 to 14 days.

The response of the stratospheric ozone concentration to solar activity was examined in different studies. A study by Angell and Korshover (1976 [11]) established a correlation of the ozone column with solar activity with a peak to peak variation up to 10 % at 70^0 latitude and only 4 % at 47^0. In the upper stratosphere there is an increasing trend of ozone with increasing solar activity. Enhanced photolysis of NO however reduces the ozone destruction during solar activity maximum. An ozone variation of 3% seems to correspond to a 20% solar UV variability at 180 nm (Keating, 1981 [156]). In general the stratospheric ozone content varies with the solar activity cycle whereas the tropospheric ozone does not. The stratospheric ozone decreases 2.72% - 3.79%, and total ozone 2,71 % - 4.36% when solar activity decreases; when solar activity increases the stratospheric ozone increases 2.41% - 3.06% and total ozone increases 2.1% - 5.56% (see Asiati *et al.*, 2004 [15]).

There seems to be no correlation of polar stratospheric temperatures and solar activity (Labitzke (1987 [179]), Labitzke, Van Loon (1988 [180]), Kerr (1988 [159]). There exists a stratospheric biennial oscillation which is more or less periodic and reversal of winds in the lower equatorial stratosphere with an average period of 27 months.

6.1.6 Troposphere

As we have seen above, only wavelengths > 300 nm penetrate to the troposphere and surface. We have already stressed that this part of the solar spectrum is only slightly variable with a peak to peak variation of about 1 part in 1400. Thus the troposphere which contains 90 % of the total mass of the Earth's atmosphere is subject to a nearly constant driving solar energy.

However, there have been innumerable attempts to find correlations between solar activity and various meteorological phenomena and other variables. If the troposphere is to be significantly influenced by the tiny changes of solar irradiation, there should exist a very strong mechanism of amplification (trigger mechanism). Such mechanisms were discussed:

- magnetospheric effects by electric field - including also effects of thunderstorms (Mc Cormac and Seliga, 1979 [215]).
- Hines (1974 [134]) suggested a change of the transmissivity of the stratosphere to upwardly propagating atmospheric waves (Callis *et al.* 1985 [52] showed from models that this is possibly not the case).
- The effect found by Labitzke (1987 [179]): temperatures in the polar winter are jointly influenced by the solar cycle and the quasi biennial oscillation and the effect on the troposphere is discussed in Van Loon and Labitzke (1988 [180]).
- Eddy (1976 [87], 1988 [88]) discussed the absence of sunspot activity during the 17th century which is known as the Maunder minimum and an earlier event, called the Spörer minimum. Both periods seem to coincide with periods of reduced global temperatures the more recent is called the Little Ice Age. Eddy (1988 [88]) showed that the required solar input reduction would have to be much greater than the tiny amplitudes detected on the time scale of a solar cycle. Maybe also amplifying factors have to be considered.

6.2 The Faint Young Sun

6.2.1 Evolution of the Solar Luminosity

According to theories of stellar evolution, the solar constant[1] is not a constant but has been increasing continuously throughout the main sequence lifetime of the Sun. The increase in luminosity can be explained by the process of energy generation inside the Sun, the nuclear fusion of hydrogen into helium; by this energy generation the mean atomic weight and density of the Sun is increased. Since the gas pressure is given by

$$P \approx kT/\mu \tag{6.5}$$

[1]The amount of energy from the Sun received per unit area at the Earth

an increase of the molecular weight μ implies a higher temperature T in order to sustain the gravity and to keep hydrostatic equilibrium. An increase in T means an increase in the energy production and thus luminosity L.

A very rough formula for the luminosity change of the Sun during its main sequence evolution was given by Gough (1981) [118]:

$$L(t) = [1 + 0.4(1 - t/t_0)]^{-1} L_0 \tag{6.6}$$

In this formula L_0 is the present solar luminosity and t_0 the present age of the Sun (4.6 Gyr). Other explanations of a possible different solar luminosity at the early evolution of the Sun are:

- Revisions in the standard solar model in order to solve the neutrino problem.
- Strong mass loss during the early phase (Willson *et al.* 1987 [335]).

Sagan and Mullen (1972) first pointed out the implications of this change of solar luminosity for the Earth's climate[2]. Using a very simple model of the greenhouse effect they showed that lower solar luminosity would have resulted in T_s below the freezing point of water for roughly the first 2 Gyr of the Earth's evolution. However this cannot be correct. Already Sagan and Mullen pointed out the presence of pillow lavas, mud cracks and ripple marks in 3.2 Gyr old rocks suggesting strongly the presence of liquid water on the Earth's surface at that time. We also know that sedimentary rocks have been deposited about 3.8 Gyrs ago and these must have formed in liquid water.

We should also stress here, that the faint young Sun was more active and variable than today, especially in the short wavelengths (X, UV).

6.2.2 Pre Main Sequence Sun

All calculations show that during the early life of the Sun, the UV flux was much higher than today. The Sun had a behavior similar to a T Tauri star. Zahnle and Walker (1982 [344]) calculated that the flux decreases as

$$\sim t^{-s} \qquad 0.5 < s < 1 \tag{6.7}$$

The exponent in this formula depends on the wavelength considered. Similar results were obtained by Canuto *et al.* (1982).

6.2.3 Albedo Variations

Let us consider the Earth to radiate like a blackbody, S is the solar constant (at present 1360 W/m^2), σ the Stefan-Boltzmann constant , A the planetary Albedo (~ 0.3), T_e the effective radiating temperature can be obtained by:

$$T_e = [S(1 - A)/4\sigma]^{1/4} \tag{6.8}$$

[2]see also e.g. The Role of the Sun in Climate Change by Douglas V. Hoyt, Kenneth H. Schatten, Kenneth H. Schatten, Oxford Univ. Press, 1997

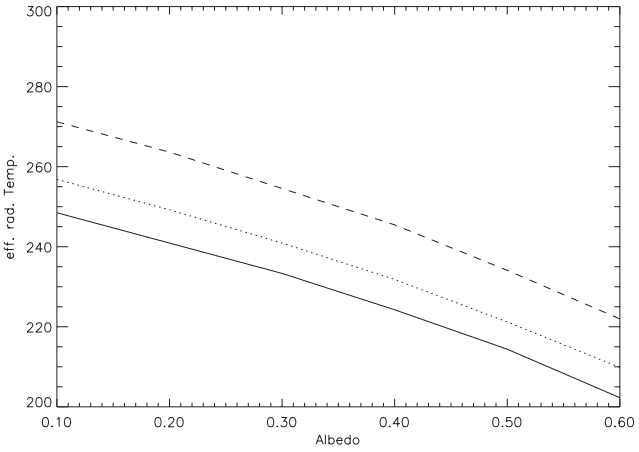

Figure 6.4: Effective radiating temperature of the Earth as a function of planetary Albedo A for three different values of the solar constant, a) 982, b) 1088 (dotted), c) present value 1360 (dashed).

The relevant albedo to use here is the *Bond Albedo*, which is the percentage of the total incident solar radiation over radiation reflected back into space. The present effective radiating temperature of the Earth is $\sim 255\,\mathrm{K}$. If we combine 6.6 and 6.8 then the increase of T_e was about 20 deg over geologic time if the albedo of the Earth is assumed to remain constant. We must also take into account the Earth's mean surface temperature T_s and

$$T_\mathrm{s} > T_\mathrm{e} \tag{6.9}$$

Because of the greenhouse effect the difference between T_s and T_e is about 33 K. The greenhouse effect is caused by the difference in opacity in the visible and infrared regions of the electromagnetic spectrum. The Earth's atmosphere is relatively transparent to incoming solar radiation, but absorbs a large fraction of the outgoing IR. Most of the absorption is caused by the vibration-rotation bands of H_2O and CO_2 and to the pure rotation band of H_2O.

In Figure 6.4 the effective radiating temperature of the earth T_e as a function of planetary albedo is given for three different values of the solar constant, a) at present b) reduced by 20 % and c) reduced by 30 %.

We clearly see that T_e strongly depends on the solar constant and on the Albedo. A larger value of the albedo leads to a lower value of the effective radiating temperature, the Earth becomes cooler. The albedo can increase because of:

- increased glaciation of the Earth,
- increased fraction of clouds.

Some typical values for A are given in Table 6.3.

Table 6.3: Typical values for the albedo.

	Albedo
Tropical forest	0.13
Woodland	0.14
Grassland	0.20
Stony desert	0.24
Sandy desert	0.37
Sea ice	0.25-0.60
Snowy ice	0.80
Cool water	<0.08
Warm water	< 0.10

One possible explanation might be that the Earth's albedo was significantly lower in the past or that the greenhouse effect of its atmosphere was larger. However, as Sagan and Mullen pointed out a large change in the Earth's albedo was unlikely; any decrease in cloudiness that might result from lower surface temperatures would likely be compensated by an increase in snow and ice cover. However if the Earth's surface was mostly water covered this argument does not work.

From climate research we know that there was no glaciation on Earth prior to about 2.7 Gyr ago (e.g. oxygen isotopes imply warm surface temperatures throughout the Precambrian (Kasting and Toon, 1989 [155])).

6.2.4 The CO_2 Geochemical Cycle

Let us start with some numbers: the total surface reservoir of carbon is about 10^{23} g. This is enough to produce a CO_2 partial pressure of about 60 bar were all of it present as gaseous (Holland, 1978). Most of the carbon is contained in carbonate rocks on the continents. A much smaller amount is present in the oceans as carbonate and bicarbonate ions (4×10^{19} g). Presently about 7×10^{17} g are present in the atmosphere (this number is growing). There is an equilibrium between the ocean and the atmosphere at timescales of about 1000 y:

CO_2 is removed from the atmosphere/ocean by weathering of silicate rocks on the continents and 20 % of atmospheric CO_2 is removed by photosynthesis followed by burial of organic carbon. If one represents silicate rocks by $CaSiO_3$ (wollastonite) then the CO_2 loss process can be described by the following three reactions:

$$CaSiO_3 + 2CO_2 + H_2O \rightarrow Ca^{++} + 2HCO_3 + SiO_2 \quad (6.10)$$

$$Ca^{++} + 2HCO_3 \rightarrow CaCO_3 + CO_2 + H_2O \quad (6.11)$$

$$(6.12)$$

Thus:

$$CaSiO_3 + CO_2 \rightarrow CaCO_3 + SiO_2 \quad (6.13)$$

When old sea floor is subducted and carbonate sediments are subjected to higher temperatures and pressures CO_2 is returned to the atmosphere/ocean. Then reaction 6.13 goes in the opposite direction, calcium silicate is reformed and gaseous CO_2 is released. Much of this CO_2 escapes through volcanoes. That process is termed carbonate metamorphism and on the young Earth the rate of carbonate metamorphism could have been augmented by faster rates of tectonic cycling and by impact processing of carbonate rich sediments.

It is important to note that the rates of the weathering reactions are strongly dependent on temperature. The reaction rates increase with temperature and weathering requires liquid water. The temperature dependence of the silicate weathering process rate leads to a negative feedback between atmospheric CO_2 and surface temperature: if the surface temperature were to decrease (because of a faint young Sun), the weathering rate would also decrease and carbon dioxide would begin to accumulate in the atmosphere. This increase of CO_2 causes an increase in the greenhouse effect and thus the temperature increases. The reverse would happen if the climate became warmer: the weathering rate would increase, pCO_2 would decrease and the greenhouse effect would become smaller (Walker *et al.* 1981 [328]). This mechanism can explain why the temperature on Earth was high enough for liquid water even when the solar luminosity was smaller.

The modern rate of CO_2 release from volcanoes would create a 1-bar CO_2 atmosphere in only 20 Myr if carbonates were not forming. This shows that the response time of the system is quite fast in geologic terms.

6.2.5 Effects of the Biota

Presently the CO_2 geochemical cycle is modulated by the biota. Calcium carbonate formation can be largely attributed to the secretion of shells by plankton and other marine organisms. Land plants enhance silicate weathering rates by pumping up the carbon dioxide partial pressure in soils by a factor of 10 to 40 over the atmospheric value; photosynthesis on land and in the oceans creates organic carbon which is then buried in sediments. Thus the atmospheric CO_2 level is reduced. Therefore, the Earth today is probably cooler than it would be in the absence of life. Lovelock (1988 [201]) created therefore the Gaia Hypothesis, which means that the Earth's climate is controlled by biota and would have become unstable where it not for the homeostatic modulation of climate by organisms. Let us assume biological control of the Earth's climate in more detail. According to Berner *et al.* [35], the dependence of the silicate weathering rate f_w on surface temperature T can be written as:

$$f_w = 1 + 0.087(T - T_0) + 0.0019(T - T_0)^2 \tag{6.14}$$

Here, T_0 is the present mean surface temperature (288 K) and $f_w = 1$. The CO_2 greenhouse effect is parameterized in the BLAG model as:

$$T - T_0 = 2.88 \ln(P/P_0) \tag{6.15}$$

where P indicates atmospheric pCO_2 and P_0 the present CO_2 partial pressure. From laboratory studies we know that the weathering rate of silicate minerals

varies approximately as

$$\mathrm{pCO}_2^{0.3} \tag{6.16}$$

for CO_2 partial pressures of 2 to 20 bar and temperatures of 100 to 200^0 C. These data were derived by Lagache (1976 [183]) and Walker *et al.* (1981 [328]). Let us assume that we can apply this relation to the Earth's surface conditions. To study the maximum effect let us further assume that removing land plants from the system would reduce surface soil pCO_2 by a factor of 40. Then the equation for the silicate weathering process can be written as:

$$\begin{aligned} f_{\mathrm{w}} &= [1 + 0.087(T - T_0) + 0.0019(T - T_0)^2] \\ &= [P_{\mathrm{S}}/40P_0)]^{0.3} \end{aligned} \tag{6.17}$$

Here P_S is the partial CO_2 pressure in the soil and today we have $P_S = 40P_0$ and obtain f_w=1. On a vegetation free Earth $P_S \sim P_0$, and f_w would be reduced by a factor of $40^{-0.3} \sim 1/3$. The carbon cycle is only balanced when $f_w = 1$. Therefore, without vegetation, the atmospheric pCO_2 and surface temperature would have to increase to bring back the silicate weathering rate to its present value. We substitute equation 6.15 into equation 6.17 and solve for P/P_0 and obtain:

$$P/P_0 = 9 \qquad T - T_0 \sim 6.3\,\mathrm{K} \tag{6.18}$$

This shows that under the assumption that land plants pump up soil CO_2 by a factor of 40, the effect of eliminating them would be to increase the Earth's temperature by only 6 deg. The net cooling effect of the biota should be somewhat larger because of the influence of the organic carbon cycle; today 20% of the carbon is organic carbon rather than carbonate. One can estimate that if life suddenly were eliminated in total the temperature would increase by 8 deg. Thus even a lifeless Earth would apparently be no warmer than the real Earth was during the Cretaceous, when the dinosaurs flourished.

The studies of Schwartzmann and Volk (1981) [275] showed that biota may accelerate chemical weathering by stabilizing soil (silicate minerals stay in contact with carbonated water), generating organic acids. This could lead to enhanced weathering rates of up to 1000 instead of 3. Therefore, the CO_2 partial pressure on a lifeless Earth might be as high as a few tenths of a bar and the surface temperature may be up to 60 K warmer!

6.2.6 T Tauri and Post T Tauri Phase

T Tauri stars are a group of stars which are solar like and often associated with molecular clouds. They are very early stars that means that they have not yet reached the main sequence and they are still contracting (see the introduction about stellar evolution). Their masses and temperatures are quite similar to the Sun but they are brighter. Their rotation rate is in the range of a few days (for the Sun it is about 1 month). They are active variable stars. The first ones were found about 1945 by their optical variability and chromospheric lines. Later on some evidence for large starspots on their surfaces were found. The X ray emission

which is about 1 000 times that of the present Sun and radio flux is not constant. Some of them also show molecular outflow and strong stellar winds. By their IR and sub mm excess radiation it was found that about half of them are surrounded by circumstellar disks.

Contrary to normal main sequence stars like the Sun their energy is not produced by nuclear fusion near the core but by a slow gravitational contraction. T Tauri stars belong to the group of so called YSO (young stellar objects) of type II. Type I YSO are very young protostellar objects at the age of just a few 100 000 years. An example is HR 4796. At a wavelength of 12 μm the object appears as a point source, at a wavelength of 21 μm it is much larger and diffuse indicating a circumstellar disk of dust. Such objects can be observed preferentially in the IR.

At an age of about 40 Million years our Sun became a zero age main sequence star. That means that it reached the main sequence and nuclear fusion of H to He started. At that time the Sun had about 70% of the total flux that is emitted presently. But in the UV and X-rays the flux was higher by a factor of about 100 than now. This of course has important consequences for the formation of the planets, their atmospheres etc. In its T Tauri and post T Tauri evolution the Sun's short wavelength emission was considerably higher than it is now. At that time the terrestrial planets were formed already, the protoplanetary disk evaporated, comets ejected out into the Oort cloud and the big bombardment period from the remaining rocky planetesimals and comets began; this caused probably several evaporations of the Earth's oceans.

How can we find indications for this T Tauri and Post T Tauri Phase of the Sun? Measurements of the ^{15}N to ^{14}N ratio in the atmosphere of the satellite Titan (which is Saturn's largest satellite) have shown that the bulk N is enhanced in the heavier ^{15}N isotope by about 4.5 times relative to the Earth's value. A ^{15}N/^{14}N anomaly on Mars of about 1.6 times the terrestrial value has also been found. These measurements can only be explained by the above mentioned T Tauri and post T Tauri phase of the early Sun (Lammer *et al.* 2000 [186]). Atmospheric sputtering and pick-up caused by a high solar wind particle outflow during a Post T-Tauri phase could be responsible for the observed nitrogen anomaly.

6.3 Solar Variability

Solar variability can be divided into three components according to their influence on the structure and composition of the atmosphere:

- variation of the solar constant
- XUV and UV variation
- energetic particle variation

So far we have only discussed the long term solar variability- summarized as the faint young Sun problem and the influence of the changing parameters of the Earth's orbit on climate (Berger, 1980 [34]).

Table 6.4: Satellite measurements of the solar constant

NIMBUS-7	16 Nov 78-13 Dec 93
SMM (ACRIM I)	16 Feb 80-01 Jun 89
ERBS	25 Oct 84-
NOAA-9	23 Jan 85-20 Dec 89
NOAA-10	22 Oct 86-01 Apr 87
UARS (ACRIM II)	5 Oct 91-
SOHO/VIRGO	18 Jan 96-

The solar input can be represented by the already mentioned solar constant S. In this context we give two interesting facts: First suppose that the Sun has no nuclear sources then the present luminosity could be maintained by a gravitational contraction of only 10^{-4} arcsec/year. Such a change would have been imperceptible over historical times. The other fact is that, as we have seen convection is a stochastic process and it is transport energy to the surface. The efficiency of convection is given by

$$l/H \tag{6.19}$$

where l is the mixing length and H the pressure scale height. Dearborn and Newman (1978) [73] show that a variation of l/H by 0.02 causes a variation of $\Delta S/S$ by 1%. Such a variation is assumed to change the global temperature on Earth by 2 K.

We now address to the question whether there exists also a variability of the solar input on shorter timescales.

6.3.1 Total Solar Irradiance Measurements

The total solar irradiance describes the radiant energy emitted by the sun over all wavelengths that falls vertically each second on 1 square meter outside the earth's atmosphere. This is the definition of the solar constant. Because of the influences of the Earth's atmosphere this constant is extremely difficult to measure on the surface and the most reliable measurements can only be done from space. In Table 6.4 the satellite measurements and the respective time spans of the measurements are summarized.

The VIRGO Experiment on the ESA/NASA SOHO Mission has two types of radiometers to measure total solar irradiance (TSI): DIARAD and PMO6V. A description of the instrument can be found in Fröhlich *et al.* (1995) [105]. Let us shortly describe the DIARAD measurement facility which is a part of SOHO/VIRGO: DIARAD is a Differential Absolute Radiometer. It is composed of two cylindrical cavities coated inside with diffuse black and mounted next to each other on the same heat sink. The flat bottom of the cavities are in fact heat flux transducers on which heating elements have been mounted. Both cavities see the same thermal environment through accurately known circular apertures.

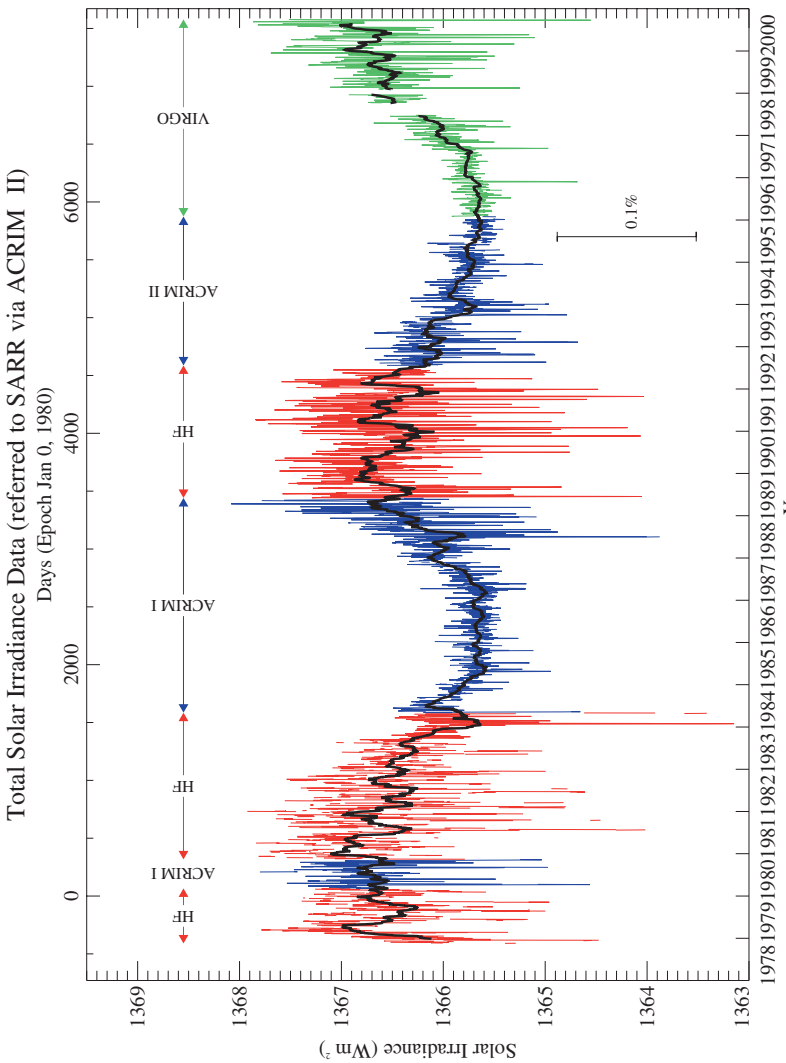

Figure 6.5: Solar irradiance measurements from satellites

A comparison of the power generated inside the cavities is done. For instance a constant electrical power is generated in one of the channels and the difference between the two heatflux sensors is automatically brought back to zero by an ad hoc accurate servosystem that provides electrical power to the other channel called "active channel". This one is regularly irradiated by the Sun or closed. The difference of the electrical power fed to the active channel when its shutter is open (exposed to the Sun) and when it is closed is proportional to the incident solar irradiance. From time to time, the roles of the left channel and the right channel are reversed for half an hour with the purpose of monitoring the aging of the continuously exposed left channel. The sampling rate of the PMO6 instrument is 1 solar total irradiance / 2 minutes, for DIARAD 1 solar total irradiance / 3 minutes.

The ACRIM contains four cylindrical bays. Three of the bays house independent heat detectors, called pyrheliometers, which are independently shuttered, self calibrating, automatically controlled, and which are uniformly sensitive from the extreme UV to the far infrared. Each pyrheliometer consists of two cavities, and temperature differences between the two are used to determine the total solar flux. One cavity is maintained at a constant reference temperature, while the other is heated 0.5 K higher than the reference cavity and is exposed to the Sun periodically. When the shutter covering the second cavity is open, sunlight enters, creating an even greater difference in cavity temperatures. The power supplied to the second cavity by the ACRIM electronics decreases automatically to maintain the 0.5 K temperature difference between the two cavities. This decrease in the amount of electricity is proportional to the solar irradiance entering the cavity. Exposing the sensors to the space environment and the Solar UV radiation causes some small changes on the surface of the cavities which may affect the measurements. The ACRIM instrument monitors this type of problem by carrying three similar sensors, two of which are normally covered. At times these are opened for comparison purposes. Further details can be found in Willson (1981 [336], 1984 [337]).

Measuring the solar constant one finds:

- Part of the energy is blocked by dark sunspots and subsequently released in faculae. The screening effect by sunspots is overcompensated by the energy storage and release. This is demonstrated in Fig. 6.6.

- There are variations of the solar constant with the solar cycle.

First measurements with the ACRIM 1 (Active Cavity Radiometer Irradiance Monitor) experiment on board the Solar Maximum Mission and the ERB experiment on the Nimbus-7 satellite showed a positive correlation between the solar cycle activity, measured by the sunspot index, and the total solar irradiance. The peak to peak variation of about 1 W/m^2 (out of about 1367) between solar maximum and minimum was reported by Fröhlich (1987) [104], Willson and Hudson (1988) [338] and Foukal and Lean (1988) [100]. Somewhat larger fluctuation up to 0.2% occur over timescales of days and weeks.

Given that the total variation between the peaks of solar cycles 21 and 22 was about 0.1%, how much is the effect to be expected for a change of the cor-

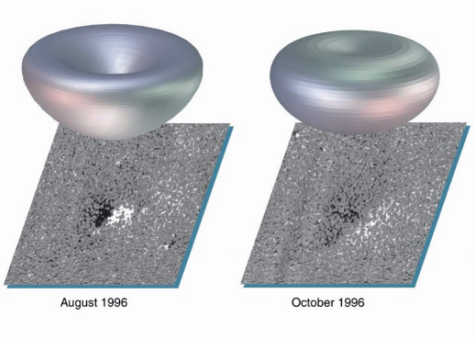

Figure 6.6: Three-dimensional rendering of the angular distribution of the excess irradiance emitted at 500 nm by the active region studied at two stages of its development, together with the magnetogram. A more uniform brightening of the facular region at the later stage is apparent (after Vicente Domingo).

responding global temperature on Earth? It is expected that this change of the solar irradiation produces a corresponding variation of about 0.2^0 C in globally averaged equilibrium surface temperature (Hansen and Lacis, 1990 [125]). But there is some considerable delay in the response. Because of the thermal inertia of the oceans, the time needed to approach equilibrium is much longer than 11 years (e.g., Reid, 1991 [254]), so that the actual temperature response to the observed variation during a solar cycle is likely to be considerably smaller, and probably insignificant from a climatic point of view.

The climate sensitivity of solar variability was studied by Scafetta and West, 2004 [271]. They estimated a solar net forcing between 10-30% of the global temperature trend between 1980 and 2002.

The complex interaction of solar variation on the atmosphere was modelled (Knipp *et al.* 2004 [169]) by using three input data:

- The solar extreme UV (XUV) power
- Joule power
- Particle kinetic power

From such a model both influences a) radiation, b) particles from the sun to the Earth can be taken into account. During 1975 and 2003 the contributions were found to be: particles 36 GW, Joule 95 GW and 464 GW for the rest. Solar wind-driven geomagnetic power provided 22% of the total global upper atmospheric energy. An interesting trend is that with increasing activity (here by the term activity short time scaled events are meant) the Joule power becomes more and more important. In the top 15 power events, geomagnetic activity contributed to 2/3 of the total power budget.

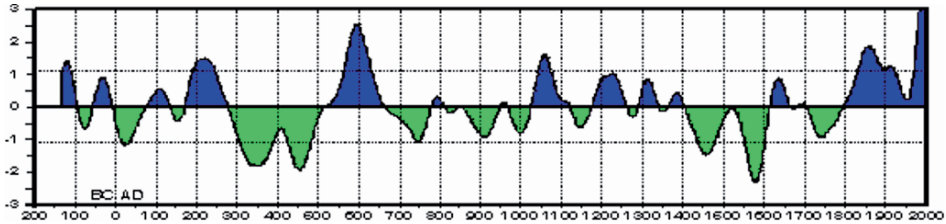

Figure 6.7: Reconstructed precipitation in northern New Mexico. Courtesy: Henri D Grissino-Mayer

6.3.2 Long Term Solar Variations

In order to study a long term variation of the solar output, there is no direct observational support. It is therefore necessary to use proxy data or solar activity indicators. Sunspot index measurements exist over a time span of roughly 350 years and they suggest the presence of a 76-80 yr cycle, the Gleissberg cycle, modulating the 11 yr cycle (Sonett, 1982 [294], Berry, 1987 [36]). Foukal and Lean (1990 [101]) gave an empirical model of total solar irradiance variation between 1874 and 1988.

The presence of the solar cycle has been claimed in various sets of proxies:

- auroral activity,
- isotopic composition of ice cores (Johnsen *et al.* 1970 [149]),
- tree growth, dendroclimatic investigations (Svenonius and Olausson, 1979 [304]). For annual rings to form, trees must "shut down" growth at some point to form a distinct ring boundary. This occurs in the dormant season, usually in the fall and winter. In the tropics, the seasons are not as distinct, so that trees can grow year-round. One fundamental principle of dendrochronology is "the present is the key to the past," originally stated by James Hutton in 1785. However, dendrochronology adds a new "twist" to this principle: "the past is the key to the future." In other words, by knowing environmental conditions that operated in the past (by analyzing such conditions in tree rings), we can better predict and/or manage such environmental conditions in the future. Hence, by knowing what the climate-tree growth relationship is in the 20th century, we can reconstruct climate from tree rings well before weather records were ever kept! Let us give one example from Grissino-Mayer: Fig 6.7 shows a long-term precipitation reconstruction for northern New Mexico based on tree rings. How this reconstruction was made? The reconstruction was developed by calibrating the widths of tree rings from the 1900s with rainfall records from the 1900s. Because we assume that conditions must have been similar in the past, we can then use the widths of tree rings as a proxy (or substitute) for actual rainfall amounts prior to the historical record.

Individual tree-growth series can be "decomposed" into an aggregate of environmental factors:

$$R_t = A_t + C_t + \Delta D1_t + \Delta D2_t + E_t \tag{6.20}$$

R_t is the tree ring growth as a function of t. A_t age related growth trend due to normal physiological aging processes, the climate (C) that occurred during that year the occurrence of disturbance factors within the forest stand (for example, a blow down of trees), indicated by $D1$, the occurrence of disturbance factors from outside the forest stand (for example, an insect outbreak that defoliates the trees, causing growth reduction), indicated by $D2$, and random (error) processes E not accounted for.

A study of tree rings and application to reconstruct climate was given by Cook *et al.* (1997). Sampling 300-to-500-year-old Siberian pine trees in the Tarvagatay Mountains of western central Mongolia, D'Arrigo *et al.*(1993 [71]) analyzed annual growth rings, which generally grow wider during warm periods and narrower in colder times in trees at the timber line. They developed a tree-ring record reflecting annual temperatures in the region dating back to 1550. The Mongolian tree rings show temperature changes that are strikingly similar to records from tree rings in North America, Europe and western Russia. The general trends reflected in the tree-ring record include cooler conditions in the early 1700s, followed by warming that started mid-century. An abrupt cooling occurred in the late 1700s and continued for much of the 1800s. The coldest period was between 1830s and 1870s, after which a steadily increasing warming trend began. An example of this analysis is given in Fig 6.8.

- Solar radius variations (Gilliland, 1981 [111]) ,
- sedimentary rocks (Sonett and Williams, 1985 [295])
- sea surface temperatures (Gerard, 1990 [107]). The mechanism how this could be related to solar irradiance variations works as follows:

  1. absorption of solar energy by the tropical oceans in a deep surface layer,
  2. transport of that energy by ocean currents,
  3. transfer of that energy by evaporation into atmospheric moisture and pressure systems leading to more precipitation (Perry, 1994 [244]).

Lewis *et al.* (1990 [195]) showed that solar radiation in visible frequencies, usually assumed to be absorbed at the sea surface, penetrates to a significant depth below the upper mixed layer of the ocean that interacts directly with the atmosphere. In clear water, the blue wavelengths, where the greatest amount of energy is available, penetrate the deepest, to nearly 100 m. Energy injected into the ocean at this depth can be stored for a substantial period of time.

As it has been stated above the transparency of the tropical oceans is dependent upon the amount of biogenic material, phytoplankton pigments, and degradation

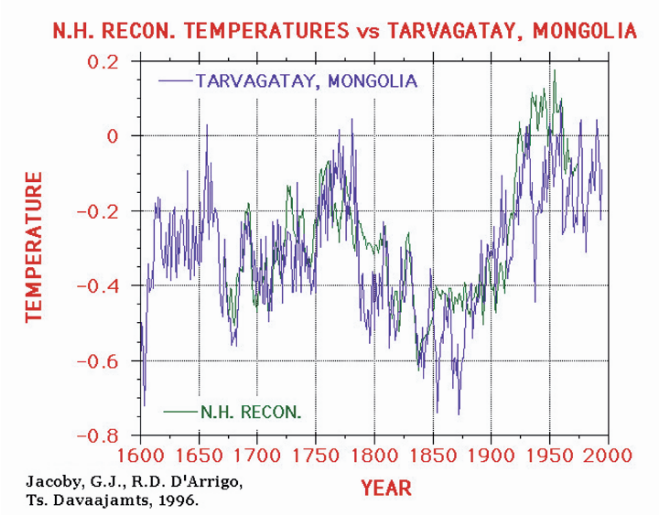

Figure 6.8: Temperatures derived from tree rings. Here the Maunder minimum is not very prominent whereas a cold period between 1830 to 1870)

products that are present. In the Pacific Ocean, transparency increases from east to west, with the greatest penetration of solar energy occurring in the western tropical Pacific. Due to ocean currents, the North Pacific Ocean takes approximately 4 years to move temperature anomalies from the western tropical Pacific to near North America (Favorite and McLain, 1973 [96]).

During the prolonged period between 1500 and 1850, average temperatures in Northern Europe were much colder than they are today, this is known as the little Ice Age. The coldest part of this period coincides with a conspicuous absence of sunspots and other signs of solar activity, called the Maunder Minimum.

For example Gilliland reported a 76 year cycle in the solar radius, inferred from a 258 year record of transits of the planet Mercury, solar eclipse records and meridian transit measurements. Ribes *et al.* (1987 [257]) also reported as Gilliland that the solar radius is slightly increased in times of low solar activity during the Maunder minimum.

A review book on the role of the Sun in climate change was written by Hoyt and Schatten (1997 [141]) where other references can be found.

Indicators of solar activity such as ^{14}C concentration measurements and of climate (e.g. glaciers) show a clear correlation over the last 7 000 years. This was shown by Eddy in 1977. Considering a time series since 1860 the solar cycle length shows an excellent correlation with northern hemisphere land temperatures (Friis-Christensen and Lassen, 1991 [103]). For recent data however, these two parameters diverge. If there exists a global climate contribution of solar irradiance variations then there are three possible interactions or couplings between these variations and the Earth's climate:

- Variations of the total solar irradiance.
- Variations of the Sun's spectral irradiance; this denotes changes in the luminosity of the Sun in a given wavelength range. As we have discussed above, UV radiation influences atmospheric chemistry (production or destruction of ozone, see also Haigh 1994 [122], 1996 [123]).
- Variations in the heliospheric magnetic field which are coupled to changes in the solar wind and influences the number and energy spectrum of cosmic ray particles. This was investigated by Potgieter, 1998 [247] and Simpson, 1998 [285]. The variation of cosmic ray particles seems to be related to global cloud cover (see Svensmark and Friis-Christensen (1997 [306]) or Svensmark (1998 [305]) or Marsch and Svensmark (2000 [211]).

As we have mentioned above, the total solar irradiance varies by 0.1% and these measurements have been made very accurately since 1978 (a review about that was given by Fröhlich, 2000 [102]) The cycles covered by these measurements are 21, 22 and 23. Of course from these time series it is impossible to extrapolate to earlier time series when the Sun was more active (e.g. cycle 19) or less active. One further problem of the time series available is that with the exception of SOHO/VIRGO they are restricted to the UV.

Irradiance variations of the past solar cycles can be determined from the surface distribution of the magnetic field if records of the field distribution or of proxies are available. The following proxies can be used:

- relative sunspot number (since 1700),
- group sunspot number (since 1610),
- sunspot and facular areas (A_s, A_f, since 1874,)
- Ca II plage areas (A_p, since 1915).

Using these data, one can reconstruct the cyclic component of the irradiance back to the Maunder minimum.

As a large sunspot group passes across the solar surface, there is a dip in the total solar irradiance. The variation is in the range of 0.02%.

Lockwood *et al.* (1999 [200]) reconstructed the aa-index of geomagnetic activity and found that the interplanetary magnetic flux at minimum of solar activity (that can be be reconstructed using the aa-index) has roughly doubled since 1900. This is in good agreement with ^{10}Be concentration in Greenland ice (Beer, 2000 [32]). ^{10}Be is produced by the interaction of cosmic rays with constituents of the Earth's atmosphere. The cosmic ray flux is modulated by the heliospheric magnetic field.

Lean *et al.* (1995 [191]) assumed that the background irradiance is proportional to the amplitude of the solar cycle; Hoyt and Schatten (1993 [140]) propose a trend corresponding to cycle length and Baliunas and Soon (1995 [25]) demonstrated that the amplitudes of stellar cycles (observed in Ca II H and K) scale with the length of the stellar cycle.

A short overview of long term chances in solar irradiance was given by Solanki and Fligge (2000 [293]).

The question whether the Earth's climate is influenced by solar activity has a central position in the present debate about the global warming. Greenhouse gas concentrations have a continuous increase and do not follow the observed decrease in the 1900's and in 1940-1970 example. These variations might be better explained when solar activity is taken into account. During a normal sunspot cycle the irradiance changes by 0.1% but could be greater (e.g. during the Maunder Minimum 0.3%, Lean (1997 [189])).

6.3.3 Solar Protons

Solar protons when hitting the atmosphere, break up molecules of N_2 and H_2O vapor. When nitrogen gas molecules split apart, they can create molecules, called nitrogen oxides NO, which can last several weeks to months depending on where they end up in the atmosphere. Once formed, the nitrogen oxides react quickly with ozone and reduce its amounts. When atmospheric winds blow them down into the middle stratosphere, they can stay there for months, and continue to keep ozone at a reduced level.

Similarly water vapor molecules are affected by solar protons, breaking them up into radicals where they react with ozone. However, these molecules, called hydrogen oxides, only last during the time period of the solar proton event. These short-term effects of hydrogen oxides can destroy up to 70 percent of the ozone in the middle mesosphere. At the same time, longer-term ozone loss caused by nitrogen oxides destroys a maximum of about nine percent of the ozone in the upper stratosphere. Only a few percent of total ozone is in the mesosphere and upper stratosphere with over 80 percent in the middle and lower stratosphere.

The impacts on humans are minimal. NASA's HALOE was launched on the UARS spacecraft September 15, 1991 as part of the Earth Science Enterprise Program. Its mission includes improvement of understanding stratospheric ozone depletion by measuring vertical profiles of ozone, hydrogen chloride, hydrogen fluoride, methane, water vapor, nitric oxide, nitrogen dioxide, aerosols, and temperature. The SBUV/2 instrument was launched aboard the NOAA-14 satellite on December 30, 1994 and its mission is to observe the ozone layer.

6.4 Cosmic Rays

6.4.1 Origination of Cosmic Rays

Victor Hess discovered in 1912 during a balloon flight to an altitude of more than 5000 m that the ionization rate increased. This fact he explained by the assumption that a radiation of very great energy penetrating power enters from above the atmosphere.[3] Energetic particles originating beyond the Earth that impinge on our atmosphere are called cosmic rays. The particles span energies

[3]Hess received the Nobel Prize in Physics in 1936

over a wide range and more than 80% are protons more than 12% He nuclei (α particles), the rest electrons, gamma rays and neutrinos. Because the particles are charged we have to take into account the interaction with magnetic fields, mainly with the heliosphere and the Earth's magnetic field. The particles are high energetic, thus they produce showers of particles when they collide with particles in our atmosphere (pions, kaons, mesons, muons).

There exist three components of cosmic rays:

- Galactic cosmic rays, GCR
- Anomalous cosmic rays, ACR
- Solar Energetic particles, SEP

Galactic Cosmic Rays

Since the particles are charged, they are deflected by the magnetic field of our Galaxy and the heliosphere as well as the Earth's magnetic field. Thus we can no longer point back to their sources in the Galaxy. A map of the sky with cosmic ray intensities would be completely uniform. The composition of the GCR's could tells us something about the origin. One finds all natural elements in roughly the same proportion as they occur in the solar system. Two properties of the particles can be measured:

- Determine which element; this is very easy since the different charges of each nucleus give different signatures.
- Isotopic composition; to determine the isotopic composition which in some cases gives better insights in the origin of the particles, the atomic nuclei have to be weighted which is much more difficult.

Most GCR are accelerated in the blast waves of supernova remnants. Remnants of supernova explosions are very active, we observe expanding clouds of gas, magnetic field activities etc. which can accelerate particles. Such processes in supernova remnants can last for several 10^3 yrs. The particles are accelerated in the magnetic field until they have enough energy to escape and become cosmic rays. Thus they can only be accelerated up to a certain maximum energy which depends upon the size of the acceleration region and the magnetic field strength.

The problem we face is that cosmic rays have been observed at much higher energies than those supernova remnants can generate. Possible explanations for such extreme high energetic particles are:

- their nature is extragalactic: from galaxies with very active galactic nuclei,
- they are related to the gamma ray bursts (energies up to 800 GeV are measured, they produce fast electrons and positrons in the Earth's atmosphere; in vacuum no particle can move faster than light. Air has a refractive index, therefore the speed of light is slowed down and fast enough electrons travel faster than light. Then, like the sonic shock ahead of a plane moving with supersonic speed they emit a shock front of light – Cherenkov radiation[4].

[4]You can see this radiation as the glow coming from a research reactor

Flashes of Cherenkov light from air showers have been studied for many years.

- they are related to exotic particles which are predicted by several physical theories concerning the origin of the universe; superstrings, exotic matter, strongly interacting neutrinos,

- they are topological defects in the very structure of the universe.

As we have stated above, cosmic rays include a number of radioactive nuclei whose numbers decrease through the radioactive decay. Measurements of these nuclei can be used therefore (as in the C^{14} method) to determine how long it has been since cosmic ray material was synthesized in the galactic magnetic field.

The origin of GCRs was discussed by Axford, 1994 [18].

One example of modern cosmic ray detectors is the Pierre Auger observatory installed in Argentina in 2005. 1600 water tanks, each containing 3000 gallons of water and separated by 1,5 km from each of its neighbors. The tanks are completely dark inside. Therefore we can measure the Cherenkov radiation of particles travelling faster than light. Slight differences in the detection times at different tank positions help scientists determine the trajectory of the incoming cosmic ray. The charged particles in an air shower also interact with atmospheric nitrogen, causing it to emit ultraviolet light via a process called fluorescence. The observatory's second detection method uses these detectors to observe the trail of nitrogen fluorescence.

Anomalous Cosmic Rays, ACR

The second component of cosmic ray particles originates from interaction with the heliosphere with neutral interstellar gas. Interstellar neutral gas flows through the solar system, since uncharged particles are not influenced by magnetic fields. The speed is approximately 25 km/s. When approaching the Sun, these neutral atoms become ionized by two processes:

- photo-ionization: an electron of the neutral atom is knocked off by a solar high energy photon (e.g. a UV photon);

- charge exchange: an electron is exchanged to an ionized atom of solar wind particle.

As soon as these particles are charged the Sun's magnetic field carries them outward to the solar wind termination shock region. The ions repeatedly collide with the termination shock, gaining energy during each collision. This continues until they escape from the shock region and diffuse back toward the inner heliosphere. Such particles are called anomalous cosmic rays (ACRs). ACRs are thought to originate from the very local interstellar medium and are not related to the above mentioned violent processes as the GCRs. They can easily be discerned from GCRs because they have lower speed and energy. They include large quantities of He, O, Ne and other elements which have in common high ionization potentials.

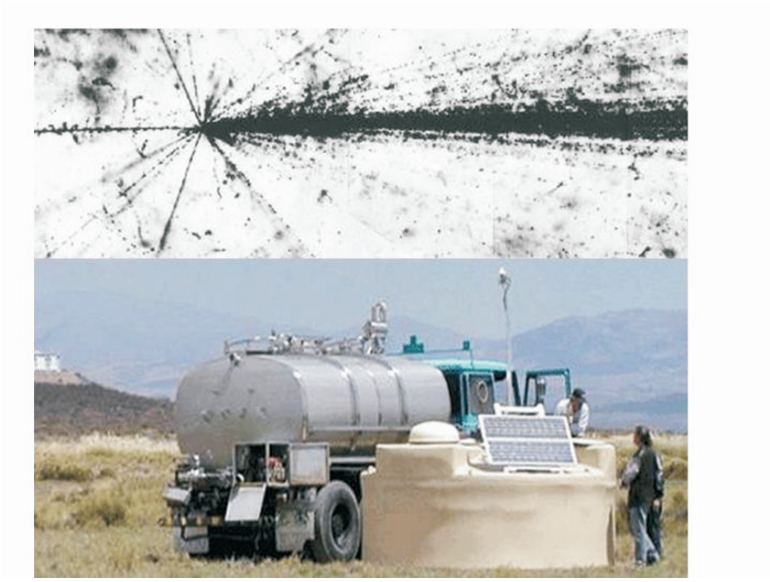

Figure 6.9: A collision between a high-energy cosmic ray particle and an atom in a photographic emulsion (viewed through a microscope). Below: filling of a water tank of the Auger observatory.

Solar Energetic Particles, SEP

The third component of cosmic ray particles are Solar energetic particles (*SEP*). They move away from the Sun due to plasma heating, acceleration and other processes. Flares e.g. inject large amounts of energetic nuclei into space, the composition varies from flare to flare. On the scale of cosmic radiation, SEPs have relatively low energies.

6.4.2 The Heliosphere

The heliosphere as already stated, is the magnetic shield caused by the Sun which protects us against energetic cosmic ray particles. The solar wind which is a continuous stream of plasma expands out through the solar system until it changes from supersonic to subsonic speed what is called a termination shock. The distance of that region is assumed to be about 90 AU and the space within is called the Heliosphere which encloses the whole solar system (e.g. Pluto's mean distance is only 39 AU). The termination shock was crossed by the spacecraft Voyager 1 on December 16, 2004 (see Stone *et al.*, 2005 [301]). The distance of the shock was at 84.01 AU from the Sun. It was found that this shock is a steady source of low energy protons. The intensity of anomalous cosmic ray helium did not peak at the shock, indicating that the ACR source is not in the shock region local to Voyager 1. The observations showed that the physics might be more complicated there. Voyager 2 is expected to cross the termination shock in 2008.

Because of the magnetic fields, only some of the GCR particles penetrate to the inner part of the solar system. Thus the magnetic field of the heliosphere works as a shield. The magnetic activity of the Sun changes however with the solar cycle (every 11 year the Sun's magnetic field reverses, the true cycle is thus 22 years). This causes a variation of the GCR flux. When the Sun is more active, the magnetic field is stronger, and as a result, fewer GCR arrive in the vicinity of the Earth. We can also say that the higher the energy the particles have, the less they are modulated by the solar cycle.

For our study here, it is important to note that by measuring cosmic rays one can derive a proxy for solar activity very long back in time. This is possible since isotopes in the atmosphere are produced by cosmic rays. From such recordings a good qualitative agreement between cold and warm climatic periods and low and high solar activity during the last 10 000 years was found. When we consider ^{14}C variations during the last millennium, one can deduce, that from 1000-1300 AC solar activity was very high which coincided with the warm medieval period. We know from history that e.g. during that period the Vikings settled in Greenland. The solar activity - if it is well represented by the ^{14}C variation- decreased and a long period followed which is now called the little ice age (in this period falls also the so called Maunder Minimum, 1645-1715, during which practically no sunspots were observed). This period lasted until the middle of the 19th century. From then on, solar activity has increased and is the highest in the last 600 years.

Thus we may assume the following connections:

$$\text{low solar activity} \rightarrow \text{weak magnetic field} \rightarrow \text{more GCRs} \rightarrow \text{more } ^{14}C \qquad (6.21)$$

If that assumption is true, there is a mechanism, how the Earth's climate can be influenced by the Sun.

The correlation between cosmic rays and solar activity and temperatures on Earth was studied by Usoskin *et al.*, 2005 [322]. Comparison of the Sun-related data sets with various reconstructions of terrestrial Northern Hemisphere mean surface temperatures reveals consistently positive correlation coefficients for the sunspot numbers and consistently negative correlation coefficients for the cosmic rays. The significance levels reach up to 99% but vary strongly for the different data sets.

Predictions of Galactic Cosmic Ray Intensity Deduced from that of Sunspot Number were made by Lantos, 2005 [188].

The relationship between cosmic ray variability and enhanced geomagnetic activity was summarized by Kudela and Storini, 2006 [178].

6.4.3 Clouds, Cloud Formation Processes

Clouds are created by condensation or deposition of water above the Earth's surface when the air mass becomes saturated (relative humidity 100 %). Saturation can occur when the temperature of an air mass goes to its dew point or frost point. There are different mechanisms to achieve this:

Orographic precipitation: this occurs when air is forced to rise because of the physical presence of elevation (land). As such a parcel of air rises it cools due to the adiabatic expansion at a rate of approximately 10 degrees per 1 000 m. The rise of the parcel is stopped if saturation is reached. An example of this mechanism is the west coast of Canada with large precipitation.

Convectional precipitation: this is associated with heating of the air at the Earth's surface. When there is enough heating, the air becomes lighter than the surrounding masses, begins to rise (cf. a hot air balloon begins to rise), expands and cools as above. When sufficient cooling takes place, saturation is reached again forming precipitation. This mechanism is active in the interior of continents and near the equator forming cumulus clouds and thunderstorms.

Convergence or frontal precipitation: this mechanism takes place when two masses of air come together. One is usually moist and warm and the other is cold and dry. The leading edge of the cold front acts as an inclined wall or front causing the moist warm air to be lifted. Then the above described processes start again: rise, cooling and saturation. This type of precipitation is common in the mid latitudes.

Finally we have to mention the radiative cooling: this occurs when the Sun is no longer supplying the ground and overlying air with energy due to insolation during nighttime. The surface of the Earth begins to lose energy in the form of longwave radiation. This causes the ground and the air above it to cool. The precipitation that results from this kind of mechanism takes the form of dew, frost or fog.

Of course these mechanisms may act as a combination: convection and orographic uplift can cause summer afternoon showers in the mountains.

Let us compare the levels of cloud cover for summer and winter (northern hemisphere). For summer in the northern hemisphere, highest levels of cloud cover occur over the mid-latitude cyclone storm tracks of both hemispheres, Intertropical Convergence Zone over land surfaces, and the Indian Monsoon region (orographic lifting). Lowest values occur over the subtropical deserts, the subsidence regions of the subtropical oceans, and the polar regions. For winter in the northern hemisphere highest levels of cloud cover occur over the mid-latitude cyclone storm tracks of both hemispheres and the Intertropical Convergence Zone over land surfaces. Lowest values occur over the subtropical deserts, the subsidence regions of the subtropical oceans, and over the South Pole.

Clouds influence vertically integrated radiative properties of the atmosphere. They cause a cooling through reflection of incoming shortwave radiation (sun - light) and heating by absorption and trapping of outgoing long wave radiation (thermal radiation). Let us consider the net radiative impact of a cloud: this mainly depends on two parameters, on its height above the surface and its optical thickness. High optically thin clouds tend to heat while low optically thick clouds tend to cool. The net forcing of the global cloud cover is in the range between $17 - 35\,\mathrm{W/m^2}$, as it is derived from climate models. Thus a significant influence on the global cloud cover can be potentially very important for Earth's climate (see also Table 6.5).

It has been found that the Earth's cloud cover follows the variation in GCR.

Table 6.5: Various influences on the climate

S, solar constant (at 1 AU)	1360 W/m^2
S/4, top of atmosphere	340 W/m^2
S/4(1-a), a=0.3 Earth's albedo	235 W/m^2
1 % change in the albedo	1 W/m^2
estimated rad. effect due to CO_2 increase since 1750	1.5 W/m^2
doubling of CO_2	4 W/m^2
radiative effect of clouds (cooling)	17-35 W/m^2

It seems to be that the ionization in the atmosphere produced by GCR is the essential link. One can estimate that a variation in cloud cover of 3 % during an average 11-year solar cycle could have an effect of 0.8-1.7 W/m^2. This is a very significant amount.

The idea that cosmic rays can influence cloud formation was first pointed out by Svensmark *et al.* (1997 [306]). They showed that there was a significant correlation between total cloud cover over the Earth and the influx of cosmic rays. The rays ionize particles in the low troposphere which then seed the growth of cloud water droplets. During the past century the shielding from cosmic rays has increased since solar activity has increased. This decreases the formation and cooling influence of low clouds and may thus provide a possible contribution to the global warming of the past 100 years (Marsh, Svensmark, 2000 [212]).

Let us consider and summarize the changes in the magnetic field in the solar atmosphere. Shorter solar cycles facilitate a rise in the coronal source flux, longer cycles allow it to decay. The accumulation of the coronal source flux strongly depends on the rate of flux emergence in active regions. In general the peak and cycle averaged sunspot numbers are larger when cycles are shorter. Therefore, shorter cycles are associated with larger flux emergence rates, there is less time for the open flux to decay. We can state:

shorter activity cycle → increased coronal flux

The coronal source surface is where the magnetic field becomes approximately radial. This occurs at $r = 2.5R_\odot$. This surface can also be regarded as the boundary that separates the solar corona from the heliosphere. The magnetic flux threading the corona source surface is called F_s or open solar flux. If there is a rise of the flux F_s than the cosmic ray flux incident on the Earth will decrease. Lockwood and Foster (2000 [199]) estimated that the cosmic ray flux > 3 GeV was 15% larger around 1900 than it is now. As it was shown above, cosmic rays generate air ions in the sub ionospheric gap which allows current to flow in the global electric current. This connects thunderclouds with the ground via lightening.

An analysis of ISCCP D2 cloud data showed a correspondence between low cloud cover and cosmic ray flux (Palle and Butler, 2000 [242]). The authors also mentioned that the effect of increased global sea temperatures, increased aerosols and aircraft traffic on cloud formation processes should be taken into account.

Table 6.6: Causes of Global Warming of about 0.5 C, 1880-1997

Climate Forcing Factor	Est. forcing °C , 1880-1997
Solar luminosity increase	+0.25[1]
Decrease in volcanic stratospheric aerosols	+0.15[2]
Increased anthropogenic sulfate aerosols	Up to -0.1 C
Increased anthropogenic carbon aerosols	Up to + 0.1 C (offsets sulfate aerosols)
Carbon dioxide warming	+0.05 to +0.10 C
Decrease in stratospheric ozone	-0.05 C[3]
Increase in cirrus contrails from airplanes	+ 0.05 C
Urban heat island effects	+0.01 to +0.10[4]
Changing skyline effects	possibly as large as + 0.25 C
Sum total of all above forcing factor	+0.51 to 0.60 C

[1] See "The Role of the Sun in Climate Change"; also see Lean *et al.*, 1995 [191].
[2] Wu *et al.*, 1999 [341]
[3] Schwartz and Andreae 1996
[4] Balling, 1992

6.5 What Causes the Global Warming?

This is a very strong debate. In the extreme case the warming is not caused by a substantial greenhouse effect since as is shown in Table 6.6 other factors can contribute to the observed increase in temperature. However, all these estimates are estimates and should be taken with caution.

In Fig 6.10 a graph from the summary for policymakers of the report of WG 1 of the intergovernmental panel on climate change illustrates the estimated global mean radiative forcing of the climate system for the year 2000 relative to 1750. The main forcing due to CFC's is easily recognized, the influence of the Sun and its variation is marked as bad known but as more important as e.g. black carbon from fossil fuel burning.

Generally, the effect of cosmic rays seems to be important but cannot explain the whole climate warming observed during the past 100 years. The climate response to changes of cosmic ray flux was investigated by Shaviv, 2005[281]. The result can be summarized as:

- there is certainly a link between the cosmic ray flux (CRF) and solar luminosity
- the increased solar luminosity during the last 100 years lead to a decreased CRF

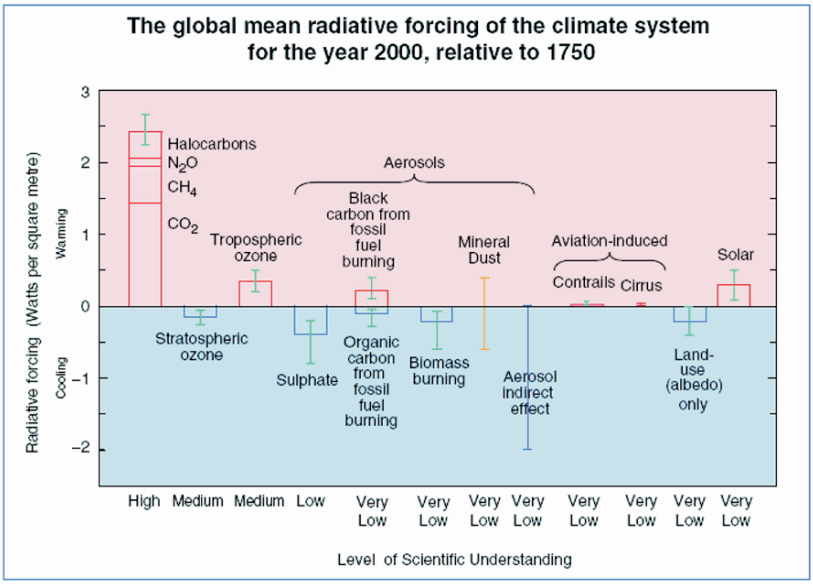

Figure 6.10: Global radiative cooling and warming of the climate system (from IPCC report).

- CRF/climate link therefore implies that the increased solar luminosity and reduced CRF over the previous century should have contributed a warming of 0.47 ± 0.19 K,
- the rest should be mainly attributed to anthropogenic causes.
- Without any effect of cosmic rays, the increase in solar luminosity would correspond to an increased temperature of 0.16 ± 0.04 K

Meteorite data on the galactic cosmic rays, the solar activity, and temperature variations in the earth's atmosphere lead to the conclusion that the solar activity may be important factor exerting the influence upon the climate of the Earth (see e.g. Alexeev, Ustinova, 2005[4]). Estimations on the long term cosmic ray variation and possible climate on planets were made by Dorman, 2005 [78].

A summary of the effects is illustrated in Fig. 6.11. The data shown in that Fig are i) Reconstructed NH temperature series from 1610-1980, updated with raw data from 1981-1995 ii) Greenhouse gases (GHG) represented by atmospheric CO2 measurements (iii) Reconstructed solar irradiance (see Lean *et al.*, 1995 [191]) (iv) Weighted volcanic dust veil index (DVI) (v) Evolving multivariate correlation of

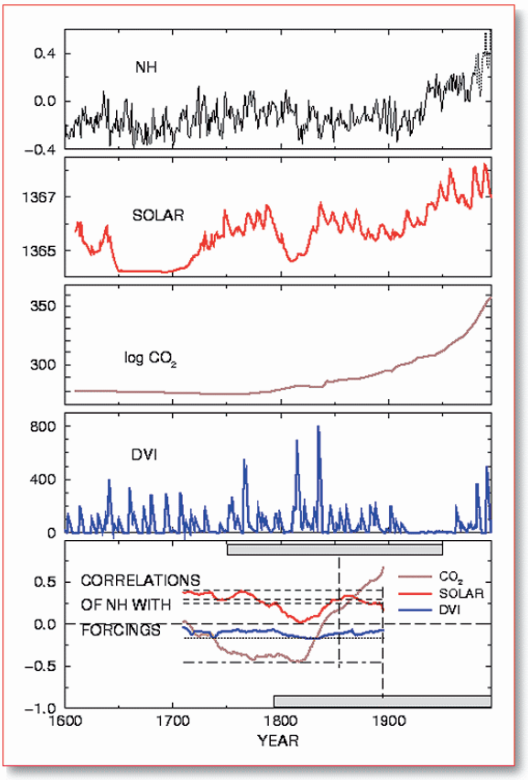

Figure 6.11: Relationship of Northern hemisphere mean (NH) temperature reconstruction to estimates of three candidate forcings between 1610 and 1995.

NH series with the 3 forcings (i) (ii) and (iii). The data are from Mann *et al.* (1999 [206], and further references therein). These authors conclude that while the natural (solar and volcanic) forcings appear to be important factors governing the natural variations of temperatures in past centuries, only human greenhouse gas forcing alone, can statistically explain the unusual warmth of the past few decades.